








# Rare variants in ANO1, encoding a calcium-activated chloride channel, predispose to moyamoya disease

Amélie Pinard,<sup>1,†</sup> Wenlei Ye,<sup>2,†</sup> Stuart M. Fraser,<sup>3</sup>  Jill A. Rosenfeld,<sup>4</sup> Pavel Pichurin,<sup>5</sup> Scott E. Hickey,<sup>6,7</sup> Dongchuan Guo,<sup>1</sup> Alana C. Cecchi,<sup>1</sup> Maura L. Boerio,<sup>1</sup> Stéphanie Guey,<sup>8</sup>  Chaker Aloui,<sup>8</sup> Kwanghyuk Lee,<sup>4</sup> Markus Kraemer,<sup>9,10</sup> Saleh Omar Alyemni,<sup>11</sup> University of Washington Center for Mendelian Genomics Michael J. Bamshad,<sup>12</sup> Deborah A. Nickerson,<sup>13,†</sup> Elisabeth Tournier-Lasserre,<sup>8,14</sup>  Shozeb Haider,<sup>11,15</sup>  Sheng Chih Jin,<sup>16,17</sup> Edward R. Smith,<sup>18</sup> Kristopher T. Kahle,<sup>19,20,21,22</sup> Lily Yeh Jan,<sup>2</sup> Mu He<sup>2,23</sup> and  Dianna M. Milewicz<sup>1</sup>

<sup>†</sup>These authors contributed equally to this work.

<sup>†</sup>Deceased.

Moyamoya disease, a cerebrovascular disease leading to strokes in children and young adults, is characterized by progressive occlusion of the distal internal carotid arteries and the formation of collateral vessels. Altered genes play a prominent role in the aetiology of moyamoya disease, but a causative gene is not identified in the majority of cases. Exome sequencing data from 151 individuals from 84 unsolved families were analysed to identify further genes for moyamoya disease, then candidate genes assessed in additional cases (150 probands). Two families had the same rare variant in ANO1, which encodes a calcium-activated chloride channel, anoctamin-1. Haplotype analyses found the families were related, and ANO1 p.Met658Val segregated with moyamoya disease in the family with an LOD score of 3.3. Six additional ANO1 rare variants were identified in moyamoya disease families.

The ANO1 rare variants were assessed using patch-clamp recordings, and the majority of variants, including ANO1 p.Met658Val, displayed increased sensitivity to intracellular Ca<sup>2+</sup>. Patients harbouring these gain-of-function ANO1 variants had classic features of moyamoya disease, but also had aneurysm, stenosis and/or occlusion in the posterior circulation.

Our studies support that ANO1 gain-of-function pathogenic variants predispose to moyamoya disease and are associated with unique involvement of the posterior circulation.

- 1 Department of Internal Medicine, Division of Medical Genetics, McGovern Medical School, University of Texas Health Science Center at Houston, Houston, TX 77030, USA
- 2 Howard Hughes Medical Institute, Department of Physiology, University of California San Francisco, San Francisco, CA 94158, USA
- 3 Department of Pediatrics, Division of Child Neurology, McGovern Medical School, University of Texas Health Science Center at Houston, Houston, TX 77030, USA
- 4 Department of Molecular and Human Genetics, Baylor College of Medicine, Houston, TX 77030, USA
- 5 Department of Clinical Genomics, Mayo Clinic, Rochester, MN 55902, USA
- 6 Department of Pediatrics, The Ohio State University, Columbus, OH 43210, USA
- 7 Division of Genetic and Genomic Medicine, Nationwide Children's Hospital, Columbus, OH 43205, USA
- 8 Université de Paris, Inserm U1141, AP-HP Groupe hospitalier Lariboisière Saint Louis, 75019 Paris, France
- 9 Department of Neurology, Alfried Krupp-Hospital, 45131 Essen, Germany

Received January 05, 2023. Revised March 24, 2023. Accepted April 16, 2023. Advance access publication May 30, 2023

© The Author(s) 2023. Published by Oxford University Press on behalf of the Guarantors of Brain. All rights reserved. For permissions, please e-mail: journals.permissions@oup.com

- 10 Department of Neurology, Medical Faculty, Heinrich-Heine-University, 40225 Düsseldorf, Germany  
11 UCL School of Pharmacy, Bloomsbury, London WC1N 1AX, UK  
12 Division of Genetics Medicine, Department of Pediatrics, University of Washington, Seattle, WA 98195, USA  
13 Department of Genome Sciences, University of Washington, Seattle, WA 98195, USA  
14 AP-HP, Service de génétique moléculaire neurovasculaire, Centre de Référence des Maladies Vasculaires Rares du Cerveau et de l'oeil, Groupe Hospitalier Saint-Louis Lariboisière, 75010 Paris, France  
15 UCL Centre for Advanced Research Computing, University College London, London WC1H 9RN, UK  
16 Department of Genetics, Washington University School of Medicine, St Louis, MO 63110, USA  
17 Department of Pediatrics, Washington University School of Medicine, St Louis, MO 63110, USA  
18 Department of Neurosurgery, Boston Children's Hospital, Harvard Medical School, Boston, MA 02115, USA  
19 Department of Neurosurgery, Yale University School of Medicine, New Haven, CT 06510, USA  
20 Department of Neurosurgery, Massachusetts General Hospital and Harvard Medical School, Boston, MA 02114, USA  
21 Broad Institute of Harvard and MIT, Cambridge, MA 02142, USA  
22 Division of Genetics and Genomics, Boston Children's Hospital, Boston, MA 02115, USA  
23 School of Biomedical Sciences, The University of Hong Kong, Pok Fu Lam, Hong Kong SAR, China

Correspondence to: Dianna M. Milewicz  
6431 Fannin St., MSB 6.100, Houston, TX 77030, USA  
E-mail: dianna.m.milewicz@uth.tmc.edu

**Keywords:** stroke genetics; smooth muscle cells; genetic heterogeneity; pathogenesis; genotype-phenotype

## Introduction

Moyamoya disease (MMD) is a progressive cerebrovascular arteriopathy characterized by bilateral stenosis or occlusion of the distal internal carotid arteries and formation of compensatory collateral vessels at the base of the brain.<sup>1</sup> MMD predisposes to ischaemic or haemorrhagic strokes with two incidence peaks of onset, one in children around 10 years of age and another in adults 30–40 years of age.<sup>1</sup> Occlusive lesions in the large arteries of MMD patients are characterized by neointimal proliferations of cells that fill the lumen and stain for smooth muscle cell (SMC) markers but lack lipid and inflammatory cell deposition typical of atherosclerotic plaques.<sup>1,2</sup>

Genetic variants are a major risk factor for MMD. Seven to twelve per cent of MMD probands have similarly affected family members.<sup>1</sup> There is an increased incidence of MMD in East Asian countries due to a founder variant in *RNF213*, p.Arg4810Lys (MIM 607151). Furthermore, rare pathogenic variants in a number of genes increase the risk for MMD, either as a single gene disorder or as part of a genetic syndrome, including *NF1*, *JAG1*, *BRCC3* and *MTCP1/MTCP1NB* deletions, *GUCY1A3*, *CBL*, *SMARCAL1*, *PCNT*, *CHD4*, *CNOT3*, *SETD5*, Xq28 copy number gain and *DIAPH1*. Bilateral stenosis of the distal internal carotid arteries without collateral formation (termed 'MMD-like vascular disease') also occurs with smooth muscle dysfunction syndrome due to *ACTA2* Arg179 variants (MIM: 613834) and Grange syndrome due to biallelic *YY1AP1* loss-of-function (LoF) variants (MIM: 602531).<sup>3–5</sup>

These causative genes for MMD hint at the molecular pathogenesis for MMD, including activation of pro-proliferative pathways (*NF1*), loss of nitric oxide signalling (*GUCY1A3*), and disruption of chromatin remodelling (*YY1AP1*, *SMARCAL1*, *CHD4*, *CNOT3*, *SETD5*). Furthermore, MMD arterial pathology suggests a prominent role of SMC migration and proliferation in MMD pathogenesis,<sup>2</sup> which is further supported by the fact that a causative gene for MMD-like disease, *ACTA2*, is expressed in SMCs and not endothelial cells. Nonetheless, the pathogenesis of MMD is poorly understood, and the majority of MMD cases, especially sporadic cases, remain genetically unsolved. Discovery of additional MMD risk genes could

help illuminate disease mechanisms, enable the creation of model systems, and lead to the development of targeted therapies.

## Materials and methods

To identify additional genes for MMD, a discovery cohort of MMD probands and their affected and unaffected family members were recruited and consented for these studies, approved by the Institutional Review Board at the University of Texas Health Science Center at Houston, and medical records were extracted and diagnoses confirmed using international consensus criteria.<sup>6</sup> Exome sequencing was pursued in 84 families with one or more members with MMD, including 28 trios, six affected probands with one unaffected parent, four large families with two or more affected members, and 46 singletons, for a total of 151 exome datasets (84 probands, eight affected relatives and 59 unaffected relatives). Bioinformatics filtering of the exome sequencing data included family segregation, a CADD (GRCh37-v1.6) score >20, and a minor allele frequency <0.0001 in gnomAD (v2.1.1 controls).

## Results

The same novel variant in *ANO1* (NM\_018043.6), p.Met658Val (CADD score 23; not present in gnomAD database), segregated with MMD in two families of our cohort (Families MM001 and MM137). To determine if the two families were distantly related, 11 informative polymorphic variants within 500 kb of the *ANO1* rare variant, NC\_000011.9:g.70011597A>G (chr11, hg19), were sequenced and identity by descent (IBD) haplotypes constructed. All the affected members of Families MM001 and MM137 shared an IBD segment that included eight polymorphisms and the *ANO1* rare variant, suggesting a common ancestor for these families (Fig. 1A). A coefficient of relatedness of 0.013–0.014 was calculated between the two families, thus estimating the affected family members were second (0.03) or third cousins (0.008). Based on this estimation, a two-point linkage analysis of the *ANO1* variant

(p.Met658Val) and MMD in the combined family determined an LOD score of 3.3.

We then identified three additional families in our cohort with ANO1 rare variants, Family MM153 (p.Ser196Thr), Family MM035 (p.Arg77Gln) and Family MM184 (p.Glu459Lys) (Fig. 1). Additional MMD cohorts were also interrogated for damaging rare variants in ANO1, including a cohort from Yale of 24 probands (22 trios and two singletons) and a French cohort of 126 MMD probands and 66 relatives (13 MMD affected and 53 unaffected relatives). Identification of additional patients with ANO1 variants was also facilitated by Matchmaker Exchange Connected Nodes<sup>7</sup> (connection between MyGene2 and GeneMatcher). Three additional rare variants in ANO1 were identified in three MMD cases, two heterozygous in singletons, as well as one homozygous variant in a 12-year-old child with MMD with an affected sibling and unaffected consanguineous parents (Table 1). The variants were located throughout the protein, and five of the seven variants were absent in gnomAD (Fig. 1B and Table 1).

ANO1 encodes anoctamin-1, a calcium-activated chloride channel (CaCC) (986 amino acids) in the TMEM16 protein family, which consists of 10 mammalian homologues ('TMEM16 A-K', skipping 'I', respectively corresponding to anoctamin 1–10).<sup>8,9</sup> Anoctamin-1 is one of the two members in the TMEM16 family that functions as a dedicated CaCC. Human ANO1 has several splice isoforms, and the isoform of 26 exons with the exclusion of exon 6b is the most abundant isoform in SMCs, heart and brain<sup>10</sup> and was thus used for functional studies (ENST00000355303). Anoctamin-1 channels are homodimers, with each subunit activated independently of the other and harbouring an anion permeation pathway and 10 transmembrane (TM) helices.<sup>11</sup> Increasing concentration of intracellular Ca<sup>2+</sup> leads to Ca<sup>2+</sup> binding to two pockets on transmembrane domains 6, 7 and 8 formed by Asn(N)677–Glu(E)731–Glu(E)760 and Asn(N)680–Glu(E)728–Asp(D)764, which triggers structural changes of several transmembrane helices to allow ion transport through the pore<sup>11</sup> (Fig. 1B). Structural analysis of the human anoctamin-1 found that residues Glu170, Ser196 and Glu459 are positioned in the region that is within the intracellular cytosol (Supplementary Fig. 1A and B), whereas residues Met658, Thr740 and Arg890 are embedded within the membrane (Supplementary Fig. 1C). All of these anoctamin-1 residues are highly conserved across species. Anoctamin-1 Met658 is located at the beginning of transmembrane domain 6 (TM6) close to a disulphide bond between cysteines 651 and 656, and Thr740 in TM7 is located in the middle of the two Ca<sup>2+</sup>-binding sites.

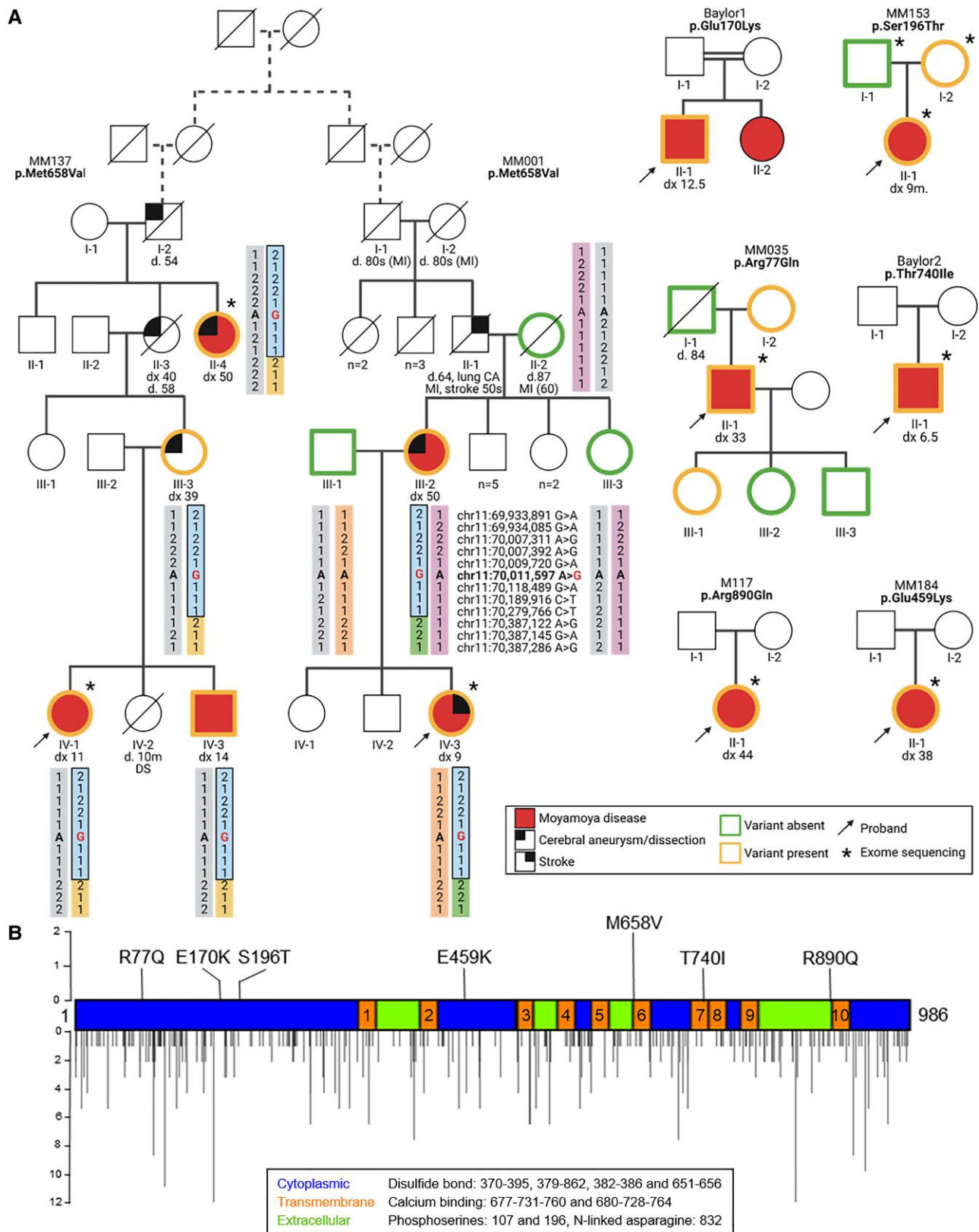
To determine if the ANO1 rare variants identified in MMD patients disrupt anoctamin-1 channel function, wild-type and mutant channels were expressed in HEK293T cells and channel function assessed using patch-clamp techniques (Fig. 2A–E). With 50 nM Ca<sup>2+</sup> in the intracellular solution, wild-type anoctamin-1 current was activated in a voltage-dependent manner, and the current-voltage relationship manifested outward rectification. In contrast, p.Met658Val, p.Glu459Lys and p.Thr740Ile anoctamin-1 were significantly different than wild-type and displayed more linearized and increased current-voltage relationships, with p.Thr740Ile having the most significant change and the highest increase of whole-cell current magnitude. Cells expressing p.Arg890Gln anoctamin-1 did not have identifiable CaCC current, and p.Arg77Gln, p.Glu170Lys and p.Ser196Thr anoctamin-1 currents were similar to wild-type.

Previous studies have shown that intracellular Ca<sup>2+</sup> concentration and membrane depolarization act synergistically to activate anoctamin-1 current.<sup>12</sup> The reduced outward rectification observed

in p.Met658Val, p.Glu459Lys and p.Thr740Ile anoctamin-1 is indicative of an increase in Ca<sup>2+</sup> affinity in these mutants, so that less membrane depolarization is required to drive Ca<sup>2+</sup> ions into the membrane electrostatic field to open the channel. We tested this hypothesis with inside-out patch-clamp recordings with the perfusion of solutions with different concentrations of Ca<sup>2+</sup> (Fig. 2F–H). Four anoctamin-1 variants, p.Met658Val, p.Glu459Lys and p.Thr740Ile, along with p.Glu170Lys, showed significantly increased Ca<sup>2+</sup> sensitivity, as can be shown in the left-shift in Ca<sup>2+</sup>-dependence traces or by the ratio of current magnitudes evoked in 50 nM Ca<sup>2+</sup> to fully-activated current amplitudes. Data from these four variants support a gain-of-function (GoF) mechanism, since cells expressing these variants have increased membrane Cl<sup>−</sup> conductance at lower intracellular Ca<sup>2+</sup> levels. The side chain of Met658 is surrounded by hydrophobic residues Ala400, Phe404, Leu657, Cys661 and Ile662. The methionine altered to the shorter side chained Val residue is predicted to be destabilizing, presumably due to the loss of tight hydrophobic packing around the pore helices (Supplementary Fig. 1D). Thus, these four ANO1 variants alter anoctamin-1 function in a similar manner, and these variants are also absent from the gnomAD database (Table 1). Cells expressing p.Arg890Gln anoctamin-1 do not have Ca<sup>2+</sup>-evoked current and loss-of-function anoctamin-1 alleles are rare in the general population (Fig. 2 and Supplementary Fig. 2). Although it appears paradoxical for both gain-of-function and loss-of-function variants to cause disease, ion channels are very tightly regulated and any perturbation in either direction could lead to altered SMC phenotype. Two N-terminal mutants (p.Arg77Gln and p.Ser196Thr) did not show changes in Ca<sup>2+</sup> sensitivity as compared to wild-type, and therefore are less likely to be disease-causing, but these two variant sites, as well as Glu170Lys, fall near the binding site for phosphatidylinositol-4,5-bisphosphate (PIP<sub>2</sub>), a constituent of plasma membrane that regulates anoctamin-1 current<sup>13,14</sup> (Fig. 2 and Supplementary Fig. 2). Thus, these variants might have allosteric effects in lipid regulation of anoctamin-1 current. It is important to note that these patch-clamp experiments were not conducted in SMCs, which limits the conclusions drawn from these results.

## Discussion

With the segregation of the gain-of-function p.Met658Val variant with MMD arguing for its causality, we assessed the MMD phenotype in all patients with ANO1 variants that increased anoctamin function. The proband of Family MM001 (IV-3 on Fig. 1A) at 9 years of age developed episodes of left-sided weakness, was diagnosed with MMD, and underwent bilateral revascularization with syngangiosis (Supplementary Table 1). MRI of the brain and magnetic resonance angiography (MRA) at 23 years old showed extensive bilateral temporal and parietal encephalomalacia, as well as bilateral occlusion of the internal carotid arteries (ICA) with robust collateral vessel formation. At 34 years of age, the patient presented with increasing left-sided weakness and numbness, and brain MRI revealed an acute right midbrain infarct in a vascular territory distinct from the surgical revascularization (Fig. 3C). Notably, MRA identified a new occlusion of the basilar artery, associated to collateral circulation from the posterior meningeal arteries, superior cerebellar arteries and posterior cerebral arteries (Fig. 3A and B). Imaging over the next 5 years revealed progressive narrowing of both the ICAs and basilar artery, with no new brain ischaemic infarcts. The proband's mother (MM001, III-2) presented with a transient ischaemic attack (TIA) at 50 years of age and an occlusive lesion was noted in the left internal carotid artery



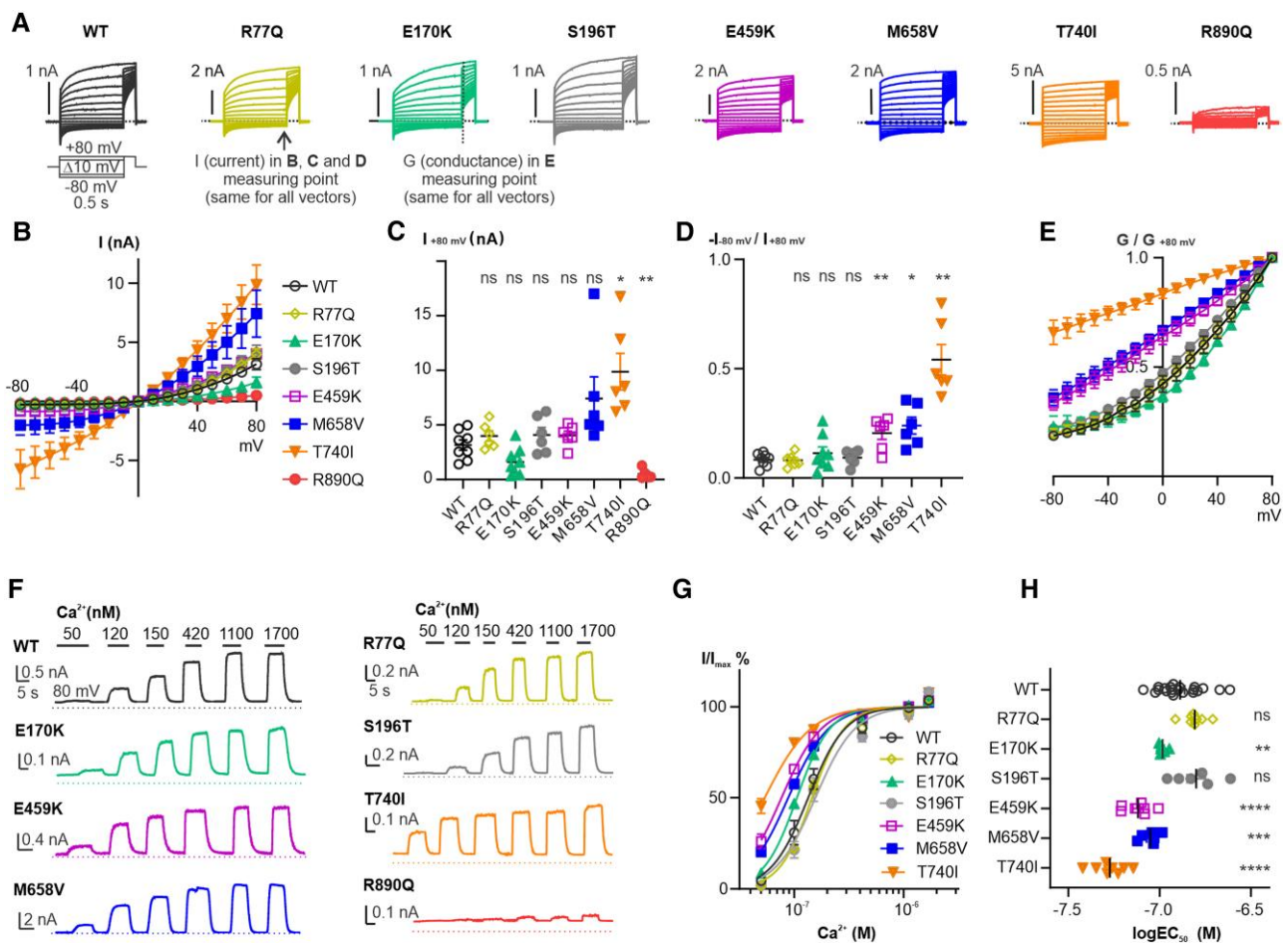
**Figure 1** Pedigrees of the families and protein map of the variants identified. (A) Pedigrees of families. Frame indicates the haplotype shared by Families MM137 and MM001. (B) Schematic representation of anoctamin-1 protein (986 amino acids), which features cytoplasmic, transmembrane and extracellular domains. Above the protein, ANO1 variants identified in this study are shown at their location on the schematic. Below the protein are rare missense and nonsense variants identified in the general population (gnomAD v2.1.1 with minor allele frequency <0.0001). Height indicates the number of individuals. CA = cancer; d. = age of death; DS = Down syndrome; dx = age of diagnosis; MI = myocardial infarct.



Table 1 Characteristics of ANO1 variants identified by exome sequencing in affected patients

Family	Chrom position (Chr11)	cDNA change	Amino acid change	Molecular effect	CADD 37-v1.6	REVEL	PolyPhen-2 v2.2.8 (HumVar)	SIFT	MAF in gnomAD v2.1.1 controls
MM035	69933979	c.230G>A	p.Arg77Gln	None	14.9	0.061	Benign	Tolerated	$2.79 \times 10^{-5}$ , (3 heterozygotes)
Baylor1	69949238	c.508G>A	p.Glu170Lys	GoF	26.1	0.691	Probably damaging	Deleterious	Not observed
MM153	69950150	c.586T>A	p.Ser196Thr	None	17.83	0.026	Benign	Tolerated	Not observed
MM184	69999184	c.1375G>A	p.Glu459Lys	GoF	26.9	0.373	Possibly damaging	Tolerated	Not observed
MM001	70011597	c.1972A>G	p.Met658Val	GoF	23	0.321	Probably damaging	Deleterious	Not observed
MM137	70011597	c.1972A>G	p.Met658Val	GoF	23	0.321	Probably damaging	Deleterious	Not observed
Baylor2	70017014	c.2219C>T	p.Thr740Ile	GoF	25.3	0.607	Probably damaging	Deleterious	Not observed
M117	70031776	c.2669G>A	p.Arg890Gln	LoF	32	0.572	Probably damaging	Deleterious	$1.09 \times 10^{-4}$ , (13 heterozygotes)

Hg19-GRCh37, ENST00000355303.9 (NM\_018043.6). GoF = gain-of-function; LoF = loss-of-function; MAF = minor allele frequency.



**Figure 2** Characterization of  $\text{Ca}^{2+}$  activated  $\text{Cl}^{-}$  current in wild-type and mutant anoctamin-1. (A) Representative traces of whole-cell currents of anoctamin-1 wild-type (WT) and mutants recorded with a voltage-family protocol from  $-80$  to  $80$  mV with increments of  $10$  mV, followed by depolarization of membrane potential to  $80$  mV, with pipette solution containing  $50$  nM  $\text{Ca}^{2+}$ . R77Q = p.Arg77Gln; E170K = p.Glu170Lys; S196T = p.Ser196Thr; E459K = p.Glu459Lys; M658V = p.Met658Val; T740I = p.Thr740Ile; R890Q = p.Arg890Gln. (B) Averaged current-voltage ( $I$ - $V$ ) relationships of WT and mutant anoctamin-1. (C) Current magnitudes measured at indicated time points at  $+80$  mV of recordings as in A. (D) Ratio of current magnitudes measured at indicated time points at  $-80$  mV to those at  $+80$  mV of recordings as in A, to indicate the rectification level of calcium-activated chloride channel (CaCC) current. R890Q was excluded from statistics due to small current amplitude. (E) Normalized conductance ( $G/G_{+80 \text{ mV}}$ ) of anoctamin-1 WT and mutants at different voltages. The conductance ratio was calculated by normalization of the current magnitudes at  $+80$  mV immediately following the voltage family protocol (intersected with the vertical dash line as in A). (F) Representative traces of inside-out recordings of anoctamin-1 WT and mutants with membrane potential held at  $+80$  mV, in response to solutions containing a series of  $\text{Ca}^{2+}$  concentrations. (G)  $\text{Ca}^{2+}$ -response curves of anoctamin-1 WT and mutants, fitted of recordings as in F with a Hill equation. (H) The logarithm of half-activation points ( $\log\text{EC}_{50}$ ) of WT and mutant anoctamin-1, calculated from fitting as in G.

(Fig. 3D), along with a basilar artery aneurysm. She underwent a left-sided synangiosis using the left temporal artery and endovascular coiling of the aneurysm. At 9 years of age, the proband of Family MM137 (IV-1) had worsening school performance, the onset of obsessive-compulsive behaviours and choreiform movements. At 11 years of age, brain MRI demonstrated T<sub>2</sub> changes in the subcortical white matter, diagnosed as silent infarcts. CT angiography demonstrated bilateral steno-occlusive lesions in the terminal ICAs, and the patient underwent revascularization with bilateral synangiosis. Her brother (MM137, IV-3) at 14 years of age had the onset of headaches and TIAs, and MRI revealed bilateral steno-occlusive lesions involving the terminal ICAs. Their mother (MM137, III-3) showed no inclusive lesions but had multiple intracranial aneurysms. The proband's grandmother (MM137, II-3) had a history of cerebral aneurysms and died at 58 years of age from an unrelated illness. At 50 years of age, her sister's (MM137, II-4) MRI found no encephalomalacia or evidence of prior strokes, but showed diffuse stenosis of the bilateral internal ICAs and a basilar tip aneurysm, which was coiled. She reported that their father died of an intracranial aneurysm rupture at 54 years of age. The patient from the family identified as Baylor 1 (II-1) presented with MMD in childhood, in association with mild supravulvular pulmonary stenosis, obesity with impaired fasting glucose and acanthosis nigricans. His family history is significant for consanguinity and a sister who also had MMD, obesity and acanthosis nigricans. The patient from Family Baylor 2 (II-1) had a history of

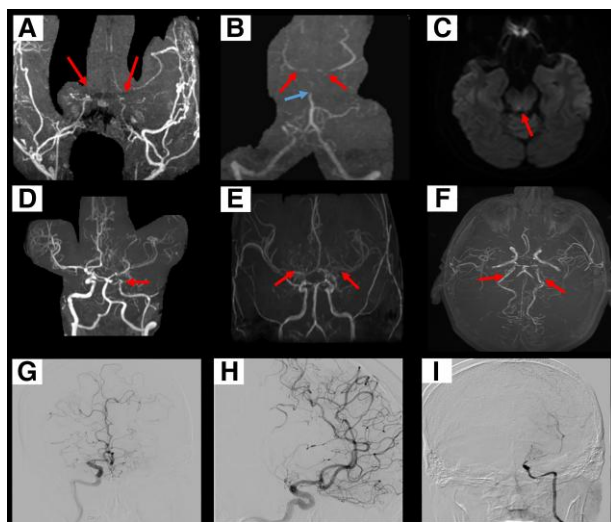


**Figure 3** Imaging of affected individuals. (A) MM001, IV-3. Magnetic resonance angiography (MRA) demonstrating bilateral internal carotid occlusion (arrows) with moyamoya vascular changes. (B) MM001, IV-3. MRA of the posterior circulation demonstrating occlusive changes of the basilar artery (blue arrow), with narrowing of bilateral posterior cerebral arteries (red arrows). (C) MM001, IV-3. Diffusion weighted MRI of the brain demonstrating a right midbrain infarct (arrow). (D) MM001, III-2. MRA demonstrating a steno-occlusion of the left internal carotid artery (ICA) with numerous pial collaterals visualized (arrow). The right internal carotid appears normal. (E) MM035, II-1. MRA demonstrating a bilateral occlusion of the supraclinoid segment of the internal carotid arteries with extensive pial collaterals (arrows). (F) MM035, II-1. MRA demonstrating bilateral stenosis of the posterior cerebral arteries (arrows). (G and H) M117, II-1. Right side middle cerebral artery (MCA) occlusion without involvement of the ICA, but with mild basal moyamoya collaterals and extensive collaterals from the posterior cerebral artery and anterior cerebral artery (ACA). (I) M117, II-1. Left side occlusion of the ACA and MCA, narrowing of the terminal part of the ICA, residual perfusion from the choroid artery, and leptomeningeal collaterals.

prematurity and intrauterine growth restriction. He presented with MMD associated with a diffuse cutis marmorata, bilateral conductive hearing loss and near-sightedness, dysmorphic features, short stature with a mild leg length discrepancy, and microcephaly. The proband of Family MM184 (II-1) was diagnosed with bilateral MMD at 38 years of age after she experienced a TIA and had bilateral vascular bypass surgery. There was no family history of MMD and her siblings were unavailable for genetic testing.

Data suggest that ANO1 may be paternally imprinted in human and mice.<sup>15</sup> In Families MM001/MM137, affected members inheriting the variant from their mother had an earlier age of onset of MMD ( $n = 3$ ; 9–14 years old), and one had three cerebral aneurysms diagnosed at 39 years of age, while affected family members who inherited the variant from their father had later onset MMD (50 years old for MM001 III-2 and MM137 II-4) (Fig. 1A).

The variant p.Arg77Gln did not alter the function of the anoctamin-1 channel, but the proband (MM035 II-1) had bilateral MMD and involvement of the posterior circulation similar to two patients above (Fig. 3E and F). The proband of Family M117 (II-1) carrying the loss-of-function variant p.Arg890Gln had an onset of stroke at 44 years of age with bilateral MMD (Fig. 3G–I). The clinical phenotype of the remainder of the cases with MMD is in the [Supplementary material](#).

We sought a connection between the gain-of-function ANO1 variants and MMD. Occluded carotid arteries from patients with MMD show neointimal lesions filled with cells that stain positive for SMC markers.<sup>2,16</sup> NF1 pathogenic variants increase the risk for MMD and SMCs explanted from *Nf1*<sup>+/-</sup> mice proliferate and migrate more rapidly than wild-type SMCs, supporting the hypothesis that increased proliferation and migration of SMCs contribute to MMD pathology.<sup>17,18</sup> ANO1 is expressed in many cell types but it is most highly expressed in arteries, particularly in the aorta<sup>19</sup> and is the only anoctamin family member expressed in cerebral artery SMCs.<sup>20</sup> ANO1 is frequently amplified in cancers and overexpression of ANO1 is correlated with poor survival.<sup>21</sup> Anoctamin-1 regulates the shape of cells, a change that is important for migration since osmotic loss of intracellular water via efflux of Cl<sup>-</sup> causes cell shrinkage and favours cell migration.<sup>22</sup> Anoctamin-1 overexpression has been shown to promote migration and invasion of cancer cells<sup>23</sup> and also non-tumour cells, such as bronchial epithelial cells.<sup>24</sup> Thus, the gain-of-function variants in ANO1, like overexpression of ANO1, potentially increase migration of SMCs. Anoctamin-1 is also important for endothelial cell function and knockdown of ANO1 increases endothelial cell proliferation and migration, so disruption of ANO1 in endothelial cells potentially contributes to MMD pathogenesis.<sup>25</sup> Multiple pharmaceutical compounds have been identified to reduce or block activity of anoctamin-1, including some approved by the FDA for treatment of non-vascular conditions,<sup>26–30</sup> and these drugs may be useful as a potential targeted therapy to prevent MMD in patients with ANO1 variants.

In summary, MMD is a poorly understood and genetically heterogeneous condition that lacks non-neurosurgical treatments. The genetic data presented strongly indicate that rare ANO1 variants, leading to increased activity of anoctamin-1 channels, predispose to MMD, along with intracranial aneurysms. These data lend further support to the proposed molecular pathogenesis of MMD as a disease due in part to pathologically increased migration of SMCs from the wall to the intima, but additional studies are needed to further validate this hypothesis. Identification of ANO1 gain-of-function variants as a cause of MMD raises the possibility of using therapeutics that block the function of anoctamin-1 to prevent MMD in these patients.

## Data availability

Most of the UTHealth exome sequencing data are available at dbGaP: phs000693.

The rest of the exome sequencing data supporting the current study have not been deposited in a public repository because it is coming from different teams from different countries but are available from the corresponding author on request.

## Web resources

MyGene2, <http://www.mygene2.org> [NHGRI/NHLBI University of Washington Center for Mendelian Genomics (UW-CMG), Seattle, WA]  
 gnomAD, <http://gnomad.broadinstitute.org/>  
 CADD, [http://cadd.gs.washington.edu/check\\_avail/v1.3\\_anno\\_73f3a82f3f9f95678ee7c661e4588902.tsv.gz](http://cadd.gs.washington.edu/check_avail/v1.3_anno_73f3a82f3f9f95678ee7c661e4588902.tsv.gz)  
 GTEx, <https://www.gtexportal.org/home/>  
 Peddy, <https://github.com/brentp/peddy>  
 IBS, <http://ibs.biocuckoo.org/online.php>  
 OMIM, <https://www.omim.org/>

## Acknowledgements

We are grateful to the patients and their family members for participating in this study. The authors would like to thank the contributors to MyGene2 and the University of Washington Center for Mendelian Genomics for use of data.

## Funding

This study was funded by an American Heart Association Merit Award (D.M.M.), the Henrietta B. and Frederick H. Bugher Foundation (D.M.M.), the Texas Heart Institute Fibromuscular Dysplasia Project (D.M.M.), the National Institutes of Health (R01NS069229 and R35NS122110; L.Y.J.), INSERM and a Fondation Leducq grant (Transatlantic Network of excellence grant 'ReVAMP-Recalibrating Mechanotransduction in Vascular Malformations' 2022–2027; E.T.-L.), and an American Heart Association Postdoctoral Fellowship (18POST34020031; A.P.). M.H. was supported by the Eunice Kennedy Shriver National Institute of Child Health and Human Development (F32HD089639). W.Y. is partially supported by the Sandler program for breakthrough biomedical research of the University of California, San Francisco. L.Y.J. is a Howard Hughes Medical Institute Investigator. Support for the Harvard team was provided by the Kids@Heart and the Caris, Doo and Marcus Chae Moyamoya Research Funds. S.O.A. is supported by the King Abdulaziz City for Science and Technology (KACST) Scholarships Program. Exome sequencing was funded by the National Human Genome Research Institute and the National Heart, Lung, and Blood Institute grant HG006493 to D.A.N., M.J.B., and Suzanne Leal. The content is solely the responsibility of the authors and does not necessarily represent the official views of the National Institutes of Health.

## Competing interests

The Department of Molecular and Human Genetics at Baylor College of Medicine receives revenue from clinical genetic testing completed at Baylor Genetics Laboratories. The other authors report no competing interests.

## Supplementary material

Supplementary material is available at *Brain* online.

## References

1. Scott RM, Smith ER. Moyamoya disease and moyamoya syndrome. *N Engl J Med*. 2009;360:1226–1237.
2. Reid AJ, Bhattacharjee MB, Regalado ES, et al. Diffuse and uncontrolled vascular smooth muscle cell proliferation in rapidly progressing pediatric moyamoya disease. *J Neurosurg Pediatr*. 2010;6:244–249.
3. Pinard A, Guey S, Guo D, et al. The pleiotropy associated with de novo variants in CHD4, CNOT3, and SETD5 extends to moyamoya angiopathy. *Genet Med*. 2020;22:427–431.
4. Kahle KT, Duran D, Smith ER. Increasing precision in the management of pediatric neurovascular diseases with molecular genetics. *J Neurosurg Pediatr*. 2023;31:228–237.
5. Mertens R, Graupera M, Gerhardt H, et al. The genetic basis of moyamoya disease. *Transl Stroke Res*. 2022;13:25–45.
6. Ferrero DM, Fullerton HJ, Bernard TJ, et al. Management of stroke in neonates and children: A scientific statement from the American Heart Association/American Stroke Association. *Stroke*. 2019;50:e51–e96.
7. Philippakis AA, Azzariti DR, Beltran S, et al. The matchmaker exchange: A platform for rare disease gene discovery. *Hum Mutat*. 2015;36:915–921.
8. Whitlock JM, Hartzell HC. Anoctamins/TMEM16 proteins: Chloride channels flirting with lipids and extracellular vesicles. *Annu Rev Physiol*. 2017;79:119–143.
9. Pedemonte N, Galletta LJ V. Structure and function of TMEM16 proteins (anoctamins). *Physiol Rev*. 2014;94:419–459.
10. Ferrera L, Caputo A, Ubbi I, et al. Regulation of TMEM16A chloride channel properties by alternative splicing. *J Biol Chem*. 2009;284:33360–33368.
11. Paulino C, Kalienkova V, Lam AKM, Neldner Y, Dutzler R. Activation mechanism of the calcium-activated chloride channel TMEM16A revealed by cryo-EM. *Nature*. 2017;552:421–425.
12. Xiao Q, Yu K, Perez-Cornejo P, Cui Y, Arreola J, Hartzell HC. Voltage- and calcium-dependent gating of TMEM16A/Ano1 chloride channels are physically coupled by the first intracellular loop. *Proc Natl Acad Sci U S A*. 2011;108:8891–8896.
13. Le SC, Jia Z, Chen J, Yang H. Molecular basis of PIP2-dependent regulation of the Ca<sup>2+</sup>-activated chloride channel TMEM16A. *Nat Commun*. 2019;10:3769.
14. Yu K, Jiang T, Cui Y, Tajkhorshid E, Hartzell HC. A network of phosphatidylinositol 4,5-bisphosphate binding sites regulates gating of the Ca<sup>2+</sup>-activated Cl<sup>-</sup> channel ANO1 (TMEM16A). *Proc Natl Acad Sci U S A*. 2019;116:19952–19962.
15. Okae H, Hiura H, Nishida Y, et al. Re-investigation and RNA sequencing-based identification of genes with placenta-specific imprinted expression. *Hum Mol Genet*. 2012;21:548–558.
16. Georgescu MM, Pinho M da C, Richardson TE, et al. The defining pathology of the new clinical and histopathologic entity ACTA2-related cerebrovascular disease. *Acta Neuropathol Commun*. 2015;3:81.
17. Lasater EA, Bessler WK, Mead LE, et al. Nf1<sup>+/-</sup> mice have increased neointima formation via hyperactivation of a Gleevec sensitive molecular pathway. *Hum Mol Genet*. 2008;17:2336–2344.
18. Xu J, Ismat FA, Wang T, Yang J, Epstein JA. NF1 Regulates a Ras-dependent vascular smooth muscle proliferative injury response. *Circulation*. 2007;116:2148–2156.
19. Manoury B, Tamuleviciute A, Tammaro P. TMEM16A/anoctamin 1 protein mediates calcium-activated chloride currents in pulmonary arterial smooth muscle cells. *J Physiol*. 2010;588:2305–2314.

20. Thomas-Gatewood C, Neeb ZP, Bulley S, et al. TMEM16A Channels generate  $\text{Ca}^{2+}$ -activated  $\text{Cl}^-$  currents in cerebral artery smooth muscle cells. *Am J Physiol Heart Circ Physiol*. 2011; 301:H1819-H1827.
21. Zhang C, Li H, Gao J, Cui X, Yang S, Liu Z. Prognostic significance of ANO1 expression in cancers. *Medicine (Baltimore)*. 2021;100:e24525.
22. Schwab A, Fabian A, Hanley PJ, Stock C. Role of ion channels and transporters in cell migration. *Physiol Rev*. 2012;92:1865-1913.
23. Wang H, Zou L, Ma K, et al. Cell-specific mechanisms of TMEM16A  $\text{Ca}^{2+}$ -activated chloride channel in cancer. *Mol Cancer*. 2017;16:152.
24. Ruffin M, Voland M, Marie S, et al. Anoctamin 1 dysregulation alters bronchial epithelial repair in cystic fibrosis. *Biochim Biophys Acta*. 2013;1832:2340-2351.
25. Ma K, Liu S, Liang H, et al.  $\text{Ca}^{2+}$ -activated  $\text{Cl}^-$  channel TMEM16A inhibition by cholesterol promotes angiogenesis in endothelial cells. *J Adv Res*. 2021;29:23-32.
26. Miner K, Labitzke K, Liu B, et al. Drug repurposing: The anthelmintics niclosamide and nitazoxanide are potent TMEM16A antagonists that fully bronchodilate airways. *Front Pharmacol*. 2019;10:51.
27. Guo S, Chen Y, Shi S, et al. Arctigenin, a novel TMEM16A inhibitor for lung adenocarcinoma therapy. *Pharmacol Res*. 2020;155: 104721.
28. Guo S, Chen Y, Pang C, et al. Matrine is a novel inhibitor of the TMEM16A chloride channel with antilung adenocarcinoma effects. *J Cell Physiol*. 2019;234:8698-8708.
29. Cottreau J, Tucker A, Crutchley R, Garey KW. Crofelemer for the treatment of secretory diarrhea. *Expert Rev Gastroenterol Hepatol*. 2012;6:17-23.
30. Tradtrantip L, Namkung W, Verkman AS. Crofelemer, an antisecretory antidiarrheal proanthocyanidin oligomer extracted from *Croton lechleri*, targets two distinct intestinal chloride channels. *Mol Pharmacol*. 2010;77:69-78.